Orientational distributions in smectic liquid crystals showing V-shaped switching investigated by polarized Raman scattering

Naoki Hayashi and Tatsuhisa Kato
Institute for Molecular Science, Myodaiji, Okazaki 444-8585, Japan

Takayuki Aoki, Tomohiro Ando, and Atsuo Fukuda
Department of Kansei Engineering, Shinshu University, Ueda 386-8567, Japan

S. S. Seomun
Department of Electronic and Electrical Engineering, Trinity College, University of Dublin, Dublin 2, Ireland
(Received 11 October 2001; published 10 April 2002)

Molecular orientational order parameters have been obtained by Raman scattering in two types of liquid crystal materials showing the V-shaped switching in thin homogeneous cells. One is the Mitsui mixture and the other is one component of the Inui mixture. The antiferroelectric phase exists in the bulk of both materials but, in thin homogeneous cells, the stability is distinct from each other. The obtained distribution of the local in-plane directors at the tip of the V is considerably broad in the former, while it is narrow in the latter. These differences have been explained by the barrier between the ferroelectric and antiferroelectric orderings, the chiral twisting power, and the interface induced destruction of the antiferroelectric ordering.

DOI: 10.1103/PhysRevE.65.041714 PACS number(s): 64.70.Md, 77.80.Fm, 78.30.Jw

I. INTRODUCTION

The electric-field-induced continuous reorientation of a spatially uniform optic axis was observed as the V-shaped switching or the thresholdless analog optical effect in two kinds of mixtures consisting of some homologues of the prototyped antiferroelectric liquid crystals, MHPOBC and TFMHPOBC [1–5], which were designated as the Inui mixture and the Mitsui mixture. This peculiar switching has attracted much attention because of its potential applications to liquid crystal displays [6–11]. The random switching model was proposed. The V-shaped switching was regarded as the Langevin-type reorientation process of local in-plane directors, the tilting directions of which are randomly distributed from smectic layer to layer. The tilting correlation of the local in-plane directors between adjacent layers was considered to be lost because of the frustration between ferroelectricity and antiferroelectricity [2–5,12]. In fact, Seomun *et al.* [13] and Pociecha *et al.* [14] confirmed that substrate interfaces destroy the antiferroelectric order in thin homogeneous cells, apparently promoting the randomization of the local in-plane directors from layer to layer. Another explanation has also been made successfully by the effective internal field model [15]. On the other hand, Takezoe *et al.* [16], Park *et al.* [17,18], Rudquist *et al.* [19], and Clark *et al.* [20] asserted the charge stabilization and/or the highly collective rotation of the local in-plane directors on the smetic-C (Sm*C**) tilt cone in the macroscopic scale, and that the frustration did not play any essential role. The polarized ir spectroscopic study indicated the almost complete director alignment parallel to a plane vertical to the substrate plates at zero electric field, which supports the collective rotation [17]. More recently, however, Seomun *et al.* showed that the alignment is not so ideal that supports the charge stabilization [21–23].

The purpose of our investigation is to understand the mechanism of the V-shaped switching. As a first step, we have established a method of elucidating the alignments of local in-plane directors at the tip of the V by utilizing polarized Raman scattering [24–28]. We have studied the molecular alignments in the two materials, one component of the Inui mixtures [compound (a)] and the Mitsui mixture (Fig. 1). In both of the materials, the antiferroelectric phase exists at low temperatures in the bulk but is not stable enough in thin homogeneous cells. The V-shaped switching is always observed at least in the high-temperature region of the antiferroelectric phase. In compound (a), however, it is stable to some extent even in thin homogeneous cells, because the tristable switching is observed in the first-run while the V-shaped switching appears in the subsequence. Some of the preliminary results were reported in the Mitsui mixture, indicating the considerably broad distribution of the local in-plane directors at the tip of the V [28]. Actually, a variety of the distributions appear to exist. The details are studied and discussed in terms of the frustration between ferroelectricity and antiferroelectricity in the following.

The paper consists of seven sections. Section II describes the experimental setups and Sec. III explains how to obtain the polarized Raman intensities as a function of sample rotation angle and to determined the apparent order parameters from the intensities. Section IV shows the experimental results of polarized Raman scattering. Section V describes the model calculations based on three types of orientational in-plane director distributions, which are consistent with some experimental results. Section VI discusses the origin of the V-shaped switching and Sec. VII gives the conclusions.

II. EXPERIMENT

Homogeneous cells of compound (a) and the Mitsui mixture listed in Fig. 1 were prepared by sandwiching the

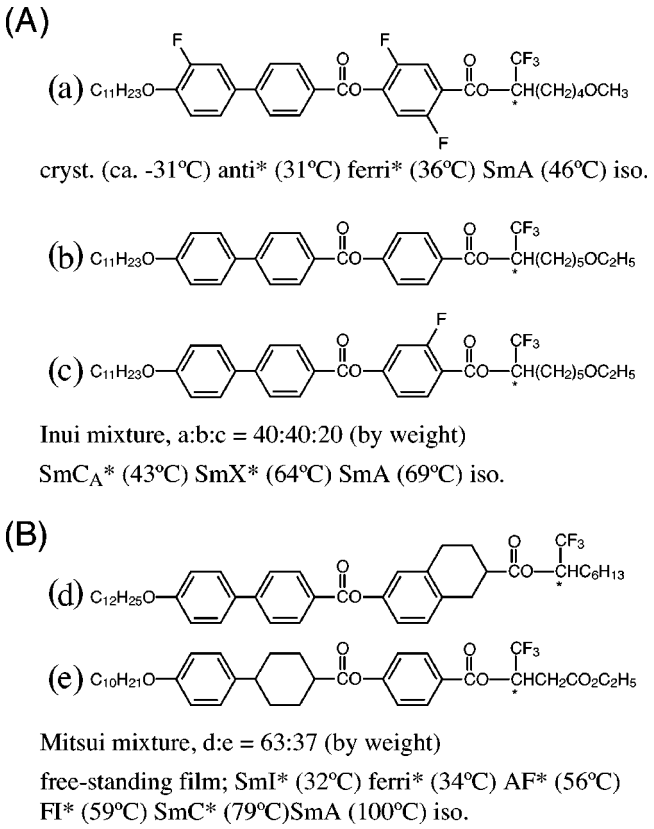

FIG. 1. Chemical structures and phase sequences of (A) Inui mixture, (B) Mitsui mixture, and compound (a).

sample between two quartz substrates separated by spacer particles of 2 μm in diameter. The substrates were coated with indium tin oxide ($\sim$50 nm thick, $\sim$100 Ω/sq, $\sim$80% transmission at 500 nm) and aligning polyimide (Nissan Chemical, RN-1266, $\sim$200 nm thick). The polyimide was carefully chosen to avoid the excess heating due to laser light absorption [22]. The only one of the substrates was rubbed in one direction and sense. The cell was mounted in a temperature-controlled oven ($\pm$0.1 K). The texture was monitored with a polarizing optical microscope (Olympus, BX50) for checking the alignment quality in each phase.

Raman spectra were obtained in the backward scattering geometry along the *Y* axis perpendicular to the substrate plates [27,28]. The *Z*- and *X*-polarized Raman intensities, $I_{Z,\mathrm{meas}}$ and $I_{X,\mathrm{meas}}$, due to the C-C stretching mode of three benzene rings with a frequency of 1600 cm^{-1} were obtained by rotating the sample cell from 0° to 180° about the *Y* axis. Here the *X*, *Y*, and *Z* axes constitute the right-handed laboratory frame. The green light at 514.5 nm from an Ar ion laser (Spectra-Physics, BeamLok 2060) was used for excitation. The beam was focused on a well-aligned area of the sample cell. The diameter of a focused spot was about 700 μm. The backscattered light was collected by a telescope lens ($f=130$ mm and $f/d=1.3$) and focused on an optical fiber, which transmitted the light to a monochromator (Spex, 270M) combined with a multichannel detector (Princeton Instruments, IPDA 512). The incident laser power was set at 0.5 W and the slit width of the monochromator was 200 μm.

The V-shaped switching was obtained by applying an electric field of triangular wave form to the cell at a frequency of 1 Hz. The scattered light at the tip of the V was detected by applying gated pulses of 4 msec width to the detector. We monitored laser light passed through the cell and a polarizer that was set in the crossed Nicol configuration by a photodiode during the Raman scattering measurement, confirming the V-shaped switching.

III. ANALYSIS

Let us consider how to obtain apparent orientational order parameters, $\langle P_2(\cos\beta)\rangle_{\mathrm{app}}$ and $\langle P_4(\cos\beta)\rangle_{\mathrm{app}}$, from experimental data, $I_Z(\omega)_{\mathrm{meas}}$ and $I_X(\omega)_{\mathrm{meas}}$ [27]. Here β is an angle between the individual molecular long axis and a molecular distribution center axis and $\langle\cdots\rangle$ denotes a statistical average. When the molecular distribution is cylindrically symmetric as in Sm*A*, the *Z*- and *X*-polarized Raman scattered intensities, $I_Z(\omega)$ and $I_X(\omega)$, as a function of the rotation angle ω between the symmetry axis and the incident laser light polarization are given by

$$I_Z(\omega)=C_1(\omega)+C_2(\omega)\langle P_2(\cos\beta)\rangle+C_3(\omega)\langle P_4(\cos\beta)\rangle + C_4(\omega)R, \tag{1}$$

$$I_X(\omega)=C_5(\omega)+C_6(\omega)\langle P_2(\cos\beta)\rangle+C_7(\omega)\langle P_4(\cos\beta)\rangle - C_4(\omega)R. \tag{2}$$

Since the scattered light is collected by an objective lens, the effect of a refracting angle on the measured intensity should be taken into account [29–32]. Hence we have

$$I_{Z,\mathrm{meas}}(\omega)=\frac{I_Z(\omega)}{n_Z(\omega)^2} \tag{3}$$

and

$$I_{X,\mathrm{meas}}(\omega)=\frac{I_X(\omega)}{n_X(\omega)^2}, \tag{4}$$

where

$$n_Z(\omega)=\frac{n_z n_x}{\sqrt{n_z^2\sin^2\omega+n_x^2\cos^2\omega}} \tag{5}$$

and

$$n_X(\omega)=\frac{n_z n_x}{\sqrt{n_z^2\cos^2\omega+n_x^2\sin^2\omega}}. \tag{6}$$

Here, the *x*, *y*, and *z* axes constitute the right-handed Cartesian coordinate frame. The *y* axis is taken to be parallel to the *Y* axis, and the *z* axis is an apparent center axis of the mo-

lecular distribution. Both of the z and x axes are in the substrate plate.

The coefficients, C_1 to C_7, are described in terms of T_x (T'_x) and T_z (T'_z), the transmission coefficients of the incident (scattered) light polarized along the x and z axes, together with $a=(2\alpha_\perp+\alpha_\parallel)/3$ and $b=\alpha_\parallel-\alpha_\perp$, the average and the anisotropy of the Raman scattering tensor components, respectively, which is assumed to be uniaxial,

$$\begin{pmatrix} \alpha_\perp & & \\ & \alpha_\perp & \\ & & \alpha_\parallel \end{pmatrix}, \tag{7}$$

$$C_1=a^2T_x^2T_x'^2+\frac{4}{45}b^2T_x^2T_x'^2+\left[-2a^2T_x^2T_x'^2+\frac{b^2}{45}(-8T_x^2T_x'^2+3T_z^2T_x'^2+3T_x^2T_z'^2)\right]\cos^2\omega+\left[a^2(T_x^2T_x'^2+T_z^2T_z'^2)+\frac{b^2}{45}(4T_x^2T_x'^2-3T_z^2T_x'^2-3T_x^2T_z'^2+4T_z^2T_z'^2)\right]\cos^4\omega, \tag{8}$$

$$C_2=-\frac{2}{3}abT_x^2T_x'^2-\frac{4}{63}b^2T_x^2T_x'^2+\left[\frac{4}{3}abT_x^2T_x'^2+\frac{b^2}{63}(8T_x^2T_x'^2+3T_z^2T_x'^2+3T_x^2T_z'^2)\right]\cos^2\omega+\left[\frac{b^2}{63}(-4T_x^2T_x'^2-3T_z^2T_x'^2-3T_x^2T_z'^2+8T_z^2T_z'^2)+\frac{ab}{3}(-2T_x^2T_x'^2+4T_z^2T_z'^2)\right]\cos^4\omega, \tag{9}$$

$$C_3=\frac{3}{35}b^2T_x^2T_x'^2+\frac{b^2}{35}(-6T_x^2T_x'^2-4T_z^2T_x'^2-4T_x^2T_z'^2)\cos^2\omega+\frac{b^2}{35}(3T_x^2T_x'^2+4T_z^2T_x'^2+4T_x^2T_z'^2+8T_z^2T_z'^2)\cos^4\omega, \tag{10}$$

$$C_4=T_xT'_xT_zT'_z\cos^2\omega-T_xT'_xT_zT'_z\cos^4\omega, \tag{11}$$

$$C_5=\frac{b^2T_x^2T_z'^2}{15}+\left[a^2(T_x^2T_x'^2+T_z^2T_z'^2)+\frac{b^2}{45}(4T_x^2T_x'^2-6T_x^2T_z'^2+4T_z^2T_z'^2)\right]\cos^2\omega+\left[a^2(-T_x^2T_x'^2-T_z^2T_z'^2)+\frac{b^2}{45}(-4T_x^2T_x'^2+3T_z^2T_x'^2+3T_x^2T_z'^2-4T_z^2T_z'^2)\right]\cos^4\omega, \tag{12}$$

$$C_6=\frac{b^2T_x^2T_z'^2}{21}+\left[\frac{ab}{3}(-2T_x^2T_x'^2+4T_z^2T_z'^2)+\frac{b^2}{63}(-4T_x^2T_x'^2-6T_x^2T_z'^2+8T_z^2T_z'^2)\right]\cos^2\omega+\left[\frac{ab}{3}(2T_x^2T_x'^2-4T_z^2T_z'^2)+\frac{b^2}{63}(4T_x^2T_x'^2+3T_z^2T_x'^2+3T_x^2T_z'^2-8T_z^2T_z'^2)\right]\cos^4\omega, \tag{13}$$

and

$$C_7=-\frac{4}{35}b^2T_x^2T_z'^2+\frac{b^2}{63}(3T_x^2T_x'^2+8T_x^2T_z'^2+8T_z^2T_z'^2)\cos^2\omega+\frac{b^2}{35}(-3T_x^2T_x'^2-4T_z^2T_x'^2-4T_x^2T_z'^2-8T_z^2T_z'^2)\cos^4\omega. \tag{14}$$

The transmission coefficients are calculated by

$$T_l=\frac{2n_g}{n_g+n_l},\quad T'_l=\frac{2n_l}{n_g+n_l}, \tag{15}$$

where n_g is the refractive index of quartz substrate plates and n_l is the principal refractive index of the liquid crystal when the light is polarized along the l axis ($l=x$ or z). Here we use $n_g=1.46$, $n_x=1.5$, and $\Delta n\equiv n_z-n_x=\Delta n_0\langle P_2(\cos\beta)\rangle$ with $\Delta n_0=0.15$. The birefringence only affects the parameter, R, which is given by

$$R=c_1\left[2a^2-\frac{4}{45}b^2+\left(\frac{2}{3}ab-\frac{8}{63}b^2\right)\langle P_2(\cos\beta)\rangle-\frac{8}{35}\langle P_4(\cos\beta)\rangle\right]+c_2\left[\frac{2}{15}b^2+\frac{2}{21}b^2\langle P_2(\cos\beta)\rangle-\frac{8}{35}\langle P_4(\cos\beta)\rangle\right]. \tag{16}$$

Here c_1 and c_2 depend on sample thickness d, birefringence Δn, incident laser light wavelength λ, and scattered light wavelength λ',

$$c_1 = \sin(K_1 d)/K_1 d \tag{17}$$

and

$$c_2 = \sin(K_2 d)/K_2 d, \tag{18}$$

with

$$K_1 = \frac{2\pi\Delta n(\lambda+\lambda')}{\lambda\lambda'} \tag{19}$$

and

$$K_2 = \frac{2\pi\Delta n(\lambda-\lambda')}{\lambda\lambda'}. \tag{20}$$

Since we usually define $\omega = 0$ when the Z and z axes coincide, as we actually did in Eqs. (1)–(14), C_4 becomes zero and the birefringence effect disappears at $\omega = 0$ and $\pi/2$.

Even for an arbitrary molecular distribution, which may not be cylindrically symmetric, the apparent center axis of the molecular distribution can be still determined so that $I_Z(\omega)$ and $I_X(\omega)$ are written in the same forms as Eqs. (1) and (2), provided that $\langle P_2(\cos\beta)\rangle$ and $\langle P_4(\cos\beta)\rangle$ are regarded as the corresponding apparent ones, $\langle P_2(\cos\beta)\rangle_{\rm app}$ and $\langle P_4(\cos\beta)\rangle_{\rm app}$. The molecular orientational distributions that will be studied in this paper are not generally cylindrically symmetric; hence $\langle P_2(\cos\beta)\rangle_{\rm app}$ and $\langle P_4(\cos\beta)\rangle_{\rm app}$ will be determined by using experimentally obtained $I_{Z,\rm meas}(\omega)$ and $I_{X,\rm meas}(\omega)$. First, $(b/a)^2$ is determined from the depolarization ratio $R_{\rm iso}$ observed in the isotropic phase:

$$R_{\rm iso} \equiv I_X/I_Z = 3b^2/(45a^2+4b^2). \tag{21}$$

Next, $I_Z(\omega)$ and $I_X(\omega)$ are simultaneously fitted with Eqs. (1) and (2), where fitting parameters are $\langle P_2(\cos\beta)\rangle_{\rm app}$, $\langle P_4(\cos\beta)\rangle_{\rm app}$, and R. Note that R can be regarded as an independent fitting parameter since it contains the birefringence effect, $d\Delta n$, as well as $\langle P_2(\cos\beta)\rangle_{\rm app}$ and $\langle P_4(\cos\beta)\rangle_{\rm app}$.

IV. RESULTS

Figure 2(A) shows the Raman spectra of compound (a) at 50°C and Fig. 2(B) those of the Mitsui mixture at 110°C in the isotropic phase. The Raman line due to the C-C stretching mode of three phenyl rings at 1600 $\rm cm^{-1}$ used is well isolated from other lines. The principal axis with the largest Raman scattering tensor component, $\alpha_\parallel$, is almost parallel to the molecular long axis. Consequently, the orientational order parameters of the molecules can be determined by measuring the polarized Raman scattered intensities of the phenyl ring stretching line [27]. The depolarization ratios were 0.391 in compound (a) and 0.356 in the Mitsui mixture, respectively.

A. Compound (a)

The thin homogeneous cell of compound (a) shows a tristable electro-optic response at 26°C in the antiferroelectric phase when a dc electric field E is applied statically. Raman intensities of phenyl line, $I_{Z,\rm meas}(\Omega)$ and $I_{X,\rm meas}(\Omega)$, are plotted against the rotation angle of the sample cell in Figs. 3 (A)[(i)–(iii)]. The smectic layer normal is along the line connecting 0° to 180° in the figure. The maximum position of $I_{Z,\rm meas}(\Omega)$, Ω_0, gives the averaged molecular orientation; $\Omega = \omega + \Omega_0$. The fitting procedures described in Sec. III give the apparent order parameters as summarized in Table I(A). The maximum position points to the layer normal at $E = 0$ [Fig. 3(A), (i)], because the numbers of layers tilting to the right and to the left are identical in the antiferroelectric phase and their tilt angles are canceled out in the macroscopic average. The orientational order parameters are considerably small. When the dc field below 3.5 $\rm V/\mu m$, which is the threshold field from antiferroelectric to ferroelectric state, is applied, the maximum position of $I_{Z,\rm meas}$ scarcely tilts from the layer normal [Fig. 3(A), (ii)] but the order parameters slightly increases. This means that the local in-plane directors rotate without destroying the antiferroelectric anticlinic structure. [33,34]. When the electric field above the threshold is applied, the maximum position of $I_{Z,\rm meas}$ tilts by 28.5° from the smectic layer normal [Fig. 3(A), (iii).] The large order parameters reflect that all the local in-plane directors are oriented in one direction parallel to the substrate plates. These changes clearly indicate the tristable switching.

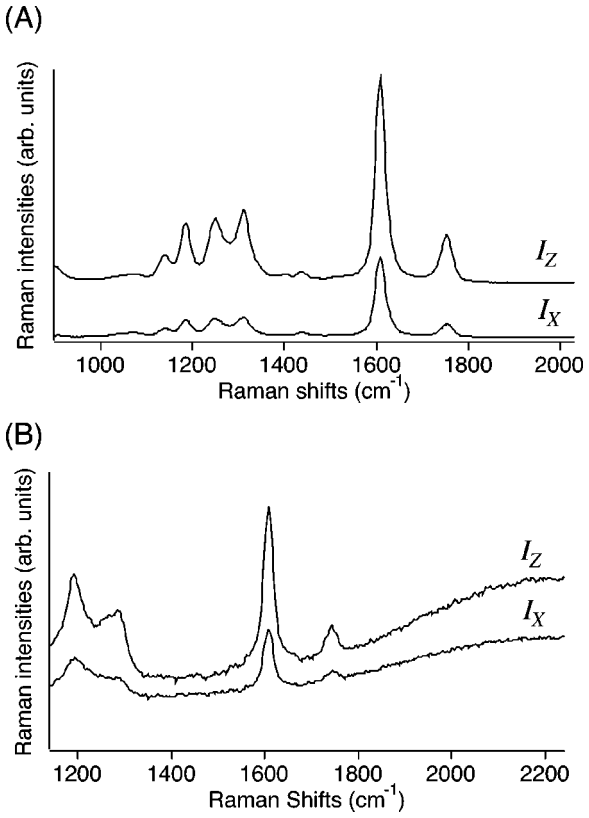

FIG. 2. Polarized Raman spectra in isotropic phase; (A) compound (a) at 50°C and (B) Mitsui mixture at 110°C.

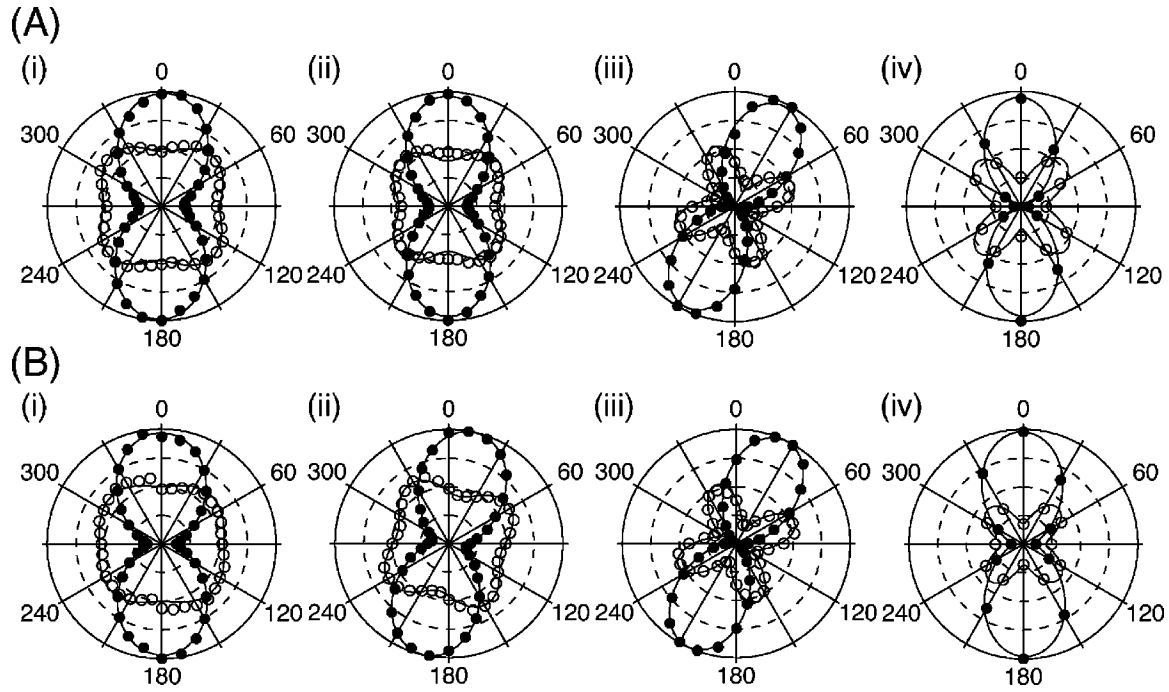

FIG. 3. Polar plots of polarized Raman scattering intensity (in arbitrary units) vs incident laser polarization (in degree) for the phenyl line. (A) Compound (a) in antiferroelectric phase at 26°C under statically applied electric fields of (i) $E=0$V, (ii) $E=2.3$ V/μm, (iii) $E=4.6$ V/μm, and (iv) at the tip of the V under dynamically applied electric field. (B) Mitsui mixture in antiferroelectric phase at 40°C under statically applied electric fields of (i) $E=0$V, (ii) $E=1.8$ V/μm, (iii) $E=5.6$ V/μm, and (iv) at the tip of the V under dynamically applied electric field. Closed and open circles represent $I_{Z,\mathrm{meas}}(\Omega)$ and $I_{X,\mathrm{meas}}(\Omega)$, respectively. The relative intensity of $I_{X,\mathrm{meas}}(\Omega)$ is enlarged by twice as compared to that of $I_{Z,\mathrm{meas}}(\Omega)$. Solid lines show the best-fitting results of Eqs. (1) and (2) with $\langle P_2(\cos\beta)\rangle_{\mathrm{app}}$ and $\langle P_4(\cos\beta)\rangle_{\mathrm{app}}$ given in Table I.

The V-shaped switching observed by applying an electric field of triangular wave form at 1 Hz is shown in Fig. 4(A), where the transmittance of light is plotted against the applied electric field. The transmittance is saturated at about 2.5 V/μm. The polarized Raman scattering was measured at the tip of the V. The intensities are plotted against the rotation angle of the sample cell in Fig. 3(A), [(iv)] as a polar plot. The molecules are oriented parallel to the layer normal as is clear in the profile of $I_{Z,\mathrm{meas}}$. The orientational order parameters are given in Table I.

TABLE I. Obtained apparent orientational order parameters; (A) compound (a) at 26°C and (B) Mitsui mixture at 40°C.

Field (V/μm)	$\langle P_2(\cos\beta)\rangle_{\mathrm{app}}$	$\langle P_4(\cos\beta)\rangle_{\mathrm{app}}$
	(A) Compound (a)	
0 (dc)	0.40 ± 0.01	-0.02 ± 0.01
2.3 (dc)	0.45 ± 0.01	0.04 ± 0.02
4.6 (dc)	0.78 ± 0.02	0.47 ± 0.04
0 (1 Hz)	0.70 ± 0.03	0.35 ± 0.05
	(B) Mitsui mixture	
0 (dc)	0.45 ± 0.01	-0.11 ± 0.01
1.8 (dc)	0.46 ± 0.01	-0.02 ± 0.01
5.6 (dc)	0.78 ± 0.01	0.48 ± 0.02
0 (1 Hz)	0.58 ± 0.03	0.20 ± 0.04

B. Mitsui mixture

The Mitsui mixture shows the V-shaped switching when a dc electric field is applied. Any macroscopic domains are not generated in this switching process. Only the extinction direction changes continuously with increasing the applied electric field.

Figures 3(B)[(i)–(iii)] are polar plots of the polarized Raman scattering intensities in the Mitsui mixture under dc electric fields at 40°C. Table I(B) summarizes the corresponding apparent order parameters. This material shows an antiferroelectric phase in the free-standing film at this temperature. At $E=0$, the maximum position of $I_{Z,\mathrm{meas}}$ points to the layer normal [Fig. 3(B), (i)] and hence the apparent tilt angle is zero. The small order parameters indicates that the surface-stabilized state is realized as in compound (a). With an increase in the applied electric field, the apparent molecular tilt angle becomes larger continuously. No threshold is observed and the transmittance shows the V-shaped switching. At $E=1.8$ V/μm, the maximum position of $I_{Z,\mathrm{meas}}$ tilts from the layer normal by 14° [Fig. 3(B), (ii)] but the order parameters, $\langle P_2(\cos\beta)\rangle_{\mathrm{app}}$ and $\langle P_4(\cos\beta)\rangle_{\mathrm{app}}$, increase only slightly as given in Table I(B). The transmittance is saturated at about 4 V/μm, where the ferroelectric state is attained. The maximum position of $I_{Z,\mathrm{meas}}$ tilts from the layer normal by 26.3° at $E=5.6$ V/μm [Fig. 3(B), (iii).]

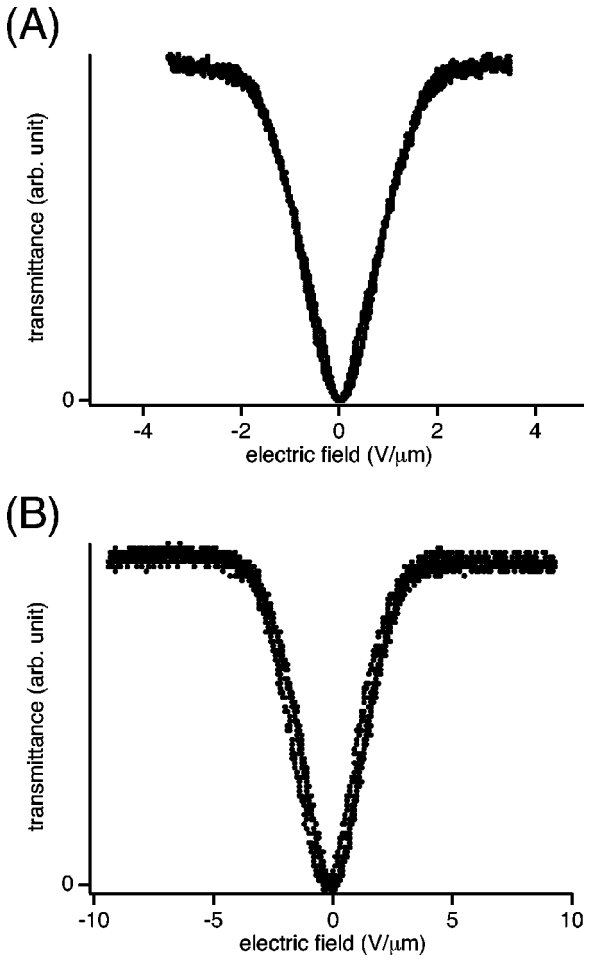

FIG. 4. Optical response under the crossed Nicol configuration when the incident laser polarization is parallel to the layer normal; (A) compound (a) at 26°C and (B) Mitsui mixture at 40°C. Transmittance of light is plotted against the applied field.

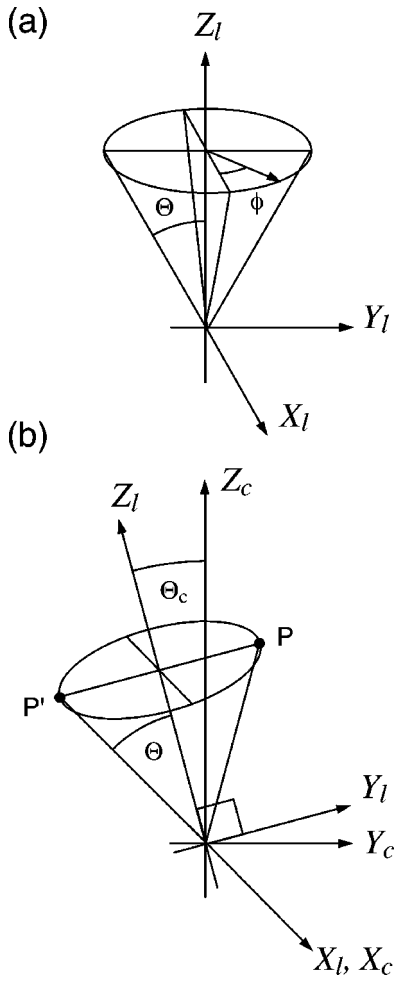

FIG. 5. Geometry with (a) bookshelf layer structure and (b) the chevron layer structure.

Figure 4(B) shows the V-shaped switching in the Mitsui mixture at 40°C when the electric field of triangular wave form is applied at 1 Hz. The transmittance saturates at about 4 V/μm as in the case of applying an dc electric field mentioned above. The polarized Raman scattering intensity measured at the tip of the V-shaped switching is shown in Fig. 3(B), [(iv)]. This profile indicates that the molecular distribution center axis is parallel to the layer normal. The fitting procedures described in Sec. III give the apparent order parameters [Table I(B).]

V. MODEL CALCULATION

To elucidate the alignment change of local in-plane directors in the switching process by polarized Raman scattering, we first presuppose some typical distributions of local in-plane directors, calculate their apparent order parameters, $\langle P_2(\cos\beta)\rangle_{\rm app}$ and $\langle P_4(\cos\beta)\rangle_{\rm app}$, and compare them with the experimentally obtained apparent order parameters. It is first assumed that the smectic layer structure is not chevron but bookshelf for the sake of simplicity. The geometry is drawn in the Fig. 5(a). The chevron structure complicates the calculations but its influence on the simulated results is relatively small as will be shown later. The following three typical distributions of local in-plane directors were assumed:

$$f_d(\phi,\theta,\chi)=\frac{1}{4\pi\sqrt{2\pi}\sigma_d}\exp\left[-\frac{(\phi-\pi/2)^2}{2\sigma_d^2}\right]\times\delta(\theta-\Theta),\quad \text{type 1} \tag{22}$$

$$f_d(\phi,\theta,\chi)=\frac{1}{8\pi\sqrt{2\pi}\sigma_d}\left\{\exp\left(-\frac{\phi^2}{2\sigma_d^2}\right)+\exp\left[-\frac{(\phi-\pi)^2}{2\sigma_d^2}\right]\right\}\delta(\theta-\Theta),\quad \text{type 2} \tag{23}$$

and

$$f_d(\phi,\theta,\chi)=\delta(\theta-\Theta)/8\pi^2,\quad \text{type 3.} \tag{24}$$

Here ϕ, θ, and χ are the Euler angles in the right-handed smectic layer frame. ϕ shows the azimuthal angle of the

TABLE II. Simulated orientational order parameters of compound (a) for the bookshelf layer structure. The molecular tilt angles used for simulations were 28.5° at 26°C and 24.7° at 32°C, which were determined experimentally by applying dc electric field above the saturation value.

		26°C		32°C	
	σ_d (°)	$\langle P_2(\cos\beta)\rangle_{\rm app}$	$\langle P_4(\cos\beta)\rangle_{\rm app}$	$\langle P_2(\cos\beta)\rangle_{\rm app}$	$\langle P_4(\cos\beta)\rangle_{\rm app}$
Type 1	0	0.70	0.38	0.64	0.30
	10	0.68	0.35	0.63	0.29
	20	0.65	0.28	0.61	0.25
Type 2	0	0.38	−0.14	0.42	−0.03
	30	0.42	−0.08	0.46	0.02
Type 3		0.50	0.04	0.51	0.09

local in-plane director and $\phi=0$ corresponds to the X_1 axis. The Z_1 axis is along the smectic layer normal and the Y_1 axis is perpendicular to the substrate plates [27]. The Y_1 and Y axes are taken to coincide each other. Type 1 is motivated by SmC^* in the Inui mixture [17–20], type 2 by surface-stabilized SmC_A^* [34], and type 3 by the random model [2,3,5,12]. These three models have symmetry axes parallel to the layer normal.

Since only the second- and fourth-order terms contribute to the Raman scattering process, the molecular orientational distribution function in the $x_E y_E z_E$ molecular orientation frame is well approximated by

$$f_{{\rm mol},E}(\alpha,\beta,\gamma)=\sum_{L=0,2,4}\frac{2L+1}{8\pi^2}\langle P_L(\cos\beta)\rangle_E P_L(\cos\beta). \tag{25}$$

Here α, β, and γ are the Euler angles in the molecular orientation frame, $\langle P_2(\cos\beta)\rangle_E$ and $\langle P_4(\cos\beta)\rangle_E$ are the apparent second- and fourth-order parameters experimentally obtained in the electric-field-induced ferroelectric SmC^* state, which result principally from molecular level fluctuations and slightly from the imperfect alignment of the smectic layers as manifested by textures. In the $X_1Y_1Z_1$ smectic layer frame, Eq. (25) can be written as [26]

$$\begin{aligned} f_{{\rm mol},E}(\phi,\theta,\chi)&=\tilde{R}(0,\Theta,0)f_{{\rm mol},E}(\alpha,\beta,\gamma)\\ &=\frac{1}{8\pi^2}\sum_{L=0,2,4}\sum_{m=-L}^{L}(2L+1)\langle P_L(\cos\beta)\rangle_E\\ &\quad\times D_{m0}^{(L)}(0,\Theta,0)D_{m0}^{(L)*}(\phi,\theta,\chi), \end{aligned} \tag{26}$$

where $D_{m0}^{(L)}(0,\Theta,0)$ is a rotation matrix, and $\tilde{R}(0,\Theta,0)$ is the rotation operator that transforms the $x_E y_E z_E$ to $X_1Y_1Z_1$-coordinate frames. Convoluting the molecular fluctuation given by Eq. (26) with one of the in-plane director distribution given by Eqs. (22)–(24), we obtain the molecular orientational distribution function

$$\begin{aligned} f_{\rm mol}(\phi,\theta,\chi)=\int_0^{2\pi}\int_0^{\pi}\int_0^{2\pi}f_d(\phi',\theta',\chi')f_{{\rm mol},E}(\phi-\phi',\theta\\ -\theta',\chi-\chi')d\phi'\sin\theta'd\theta'd\chi'. \end{aligned} \tag{27}$$

Inserting Eqs. (25) and (26) into Eq. (27), we obtain the apparent molecular orientational Lth ($L=2$ and 4) order parameters

$$\langle P_L(\cos\beta)\rangle_{\rm app}=\sum_{m=-L}^{L}\langle D_{m0}^{(L)*}(\phi,\theta,\chi)\rangle, \tag{28}$$

with

$$\begin{aligned} \langle D_{m0}^{(L)*}(\phi,\theta,\chi)\rangle=\int_0^{2\pi}\int_0^{\pi}\int_0^{2\pi}D_{m0}^{(L)*}(\phi,\theta,\chi)\\ \times f_{\rm mol}(\phi,\theta,\chi)d\phi\sin\theta\,d\theta d\chi. \end{aligned} \tag{29}$$

The results of the model calculation for compound (a) is listed in Table II. The orientational order parameters experimentally obtained at 26°C with no applied electric field are well reproduced by the result of the type 2 model with a small σ_d. Moreover, the compound (a) exhibits the tristable switching under statically applied electric field, as mentioned before. These results suggest that the usual surface-stabilized anticlinic molecular alignment without helical structure is formed. The orientational order parameters at the tip of the V are well described by the result of the type 1 with a very small σ_d. The $\langle P_2(\cos\beta)\rangle_{\rm app}$ of 0.63 ± 0.03 and $\langle P_4(\cos\beta)\rangle_{\rm app}$ of 0.27 ± 0.05 were also obtained, respectively, at the tip of the V at 32°C in the ferrielectric phase. These orientational order parameters also coincide with the result of the type 1 with a very small σ_d. Hence, for the compound (a), the small distribution at the tip of the V suggests collective rotation of the local in-plane director.

Table III summarizes the results of the model calculation for the Mitsui mixture. At 40°C with no dc field, the orientational order parameters agree with the results given by type 2 with $\sigma_d=0°$. This result suggests the surface-stabilized molecular alignment. However, the V-shaped switching in the first-run indicates that the state is not the usual antiferroelectric, anticlinic molecular alignment. The orientational order parameters at the tip of the V are described by the type 3 or the type 1 with a large σ_d. The orientational order parameters were also obtained at 60°C, where the phase was ferroelectric in a free-standing film. $\langle P_2(\cos\beta)\rangle_{\rm app}$ of 0.60 ±0.03 and $\langle P_4(\cos\beta)\rangle_{\rm app}$ of 0.12 ± 0.05 were obtained, respectively at the tip of the V. These values were well described by the type 3 (Table III). Consequently, the molecu-

TABLE III. Simulated orientational order parameters of Mitsui mixture for the bookshelf layer structure. The molecular tilt angles used for simulations were 26.3° at 40°C and 22.8° at 60°C, which were determined experimentally by applying dc electric field above the saturation value.

		40°C		60°C	
	σ_d (°)	$\langle P_2(\cos\beta)\rangle_{\rm app}$	$\langle P_4(\cos\beta)\rangle_{\rm app}$	$\langle P_2(\cos\beta)\rangle_{\rm app}$	$\langle P_4(\cos\beta)\rangle_{\rm app}$
Type 1	0	0.74	0.41	0.74	0.42
	30	0.65	0.25	0.68	0.30
	60	0.57	0.12	0.61	0.19
Type 2	0	0.43	−0.10	0.50	−0.01
	30	0.48	−0.03	0.54	0.06
Type 3		0.55	0.09	0.60	0.16

lar orientation of the Mitsui mixture at the tip of the V is characterized by the considerable large distribution of the local in-plane directors.

When the chevron structure was considered, Eq. (26) should be modified. The geometry with the chevron layer structure is drawn in Fig. 5(b). The Z_1 axis, which represents the smectic layer normal, is inclined at Θ_c from Z_c axis, which is parallel to the substrate plane. The X_c, Y_c, and Z_c axes constitute the right-handed Cartesian coordinate frame. The X_c axis is identical with the X_1 axis. When the model of the type 1 with $\sigma_d=0$ is applied to the tip of the V, the local in-plane director has two choice of either point, P or P', which are not identical now. It is reasonable to select P with the smaller inclined angle with respect to the substrate plane. The molecular distribution function was given by

$$f_c(\phi_c,\theta_c,\chi_c)=\tilde{R}(-\pi/2,\Theta_c,0)f_{\rm mol}(\phi,\theta,\chi), \qquad (30)$$

where $\tilde{R}(-\pi/2,\Theta_c,0)$ is the rotation operator that transforms the $X_1Y_1Z_1$ to the $X_cY_cZ_c$-coordinate frames. In the models of type 2 and 3, the center axis of the molecular orientational distribution, which is parallel to the layer normal, is inclined at Θ_c with respect to the substrate plane. Thus, the apparent orientational order parameters were calculated by considering the chevron layer structure in Eqs. (22)–(30). Tables IV and V show the results of the model calculation that takes into consideration the chevron structure for the compound (a) and the Mitsui mixture, respectively. The chevron angle of 15° was assumed because the angle was up to 12° [18]. $\langle P_L(\cos\beta)\rangle_E$ used for this calculation were identical with those used in the calculation with the bookshelf structure because the sufficiently high electric field induces the deformation to the bookshelf structure from the chevron structure [35]. The results showed that the chevron structure does not affect the essential understandings of the molecular distribution at the tip of the V.

Let us consider the polarization-stabilized twisted SmC^* structure proposed by Rudquist *et al.* [19]. The bookshelf structure is also presumed here. The spatial distribution of the local in-plane director along the Y_1 axis can be divided into three parts, that is, the bulk of uniform orientation structure with high coherence at $\phi=\pi/2$ in the middle of the cell and the upper and lower thin surface regions with twisted structure. As we go from one substrate to the other of the liquid crystal sample cell, ϕ increases from zero at one substrate to $\pi/2$ at the interface between the surface and bulk regions, keeps $\pi/2$ in the bulk region, and increases again from $\pi/2$ to π at the other substrate. When the joined two surface regions are supposed to be one uniform twisted structure, the distribution of the local in-plane director is given by the same function as Eq. (24) provided the distribution along the Y_1 axis instead of the Z_1 axis is considered. The distribution in the bulk region is represented by Eq. (22) with $\sigma_d=0$. The averaged distribution of the local in-plane director depends on the ratio of the surface regions in the entire space. The highest value of the apparent orientational order parameter is given in the entire bulk region of the sample cell (type 1 with σ_d in Tables II and III), and the lowest value in the entire surface regions (type 3 in Tables II and III.) This means that the apparent orientational order parameter decreases with an increase of the ratio of the surface regions to the bulk region, and vice versa. The orientational order parameters of the compound (a) at the tip of the V are well described by the type 1. This indicates that the surface regions must be sufficiently thin. On the other hand, in the case of the Mitsui mixture, the low order parameters at the tip of the V can be described by the type 3. This suggests that the

TABLE IV. Simulated orientational order parameters of compound (a) for the chevron layer structure. The chevron angle was assumed at 15°. The other parameters were identical with Table II.

		26°C		32°C	
	σ_d (°)	$\langle P_2(\cos\beta)\rangle_{\rm app}$	$\langle P_4(\cos\beta)\rangle_{\rm app}$	$\langle P_2(\cos\beta)\rangle_{\rm app}$	$\langle P_4(\cos\beta)\rangle_{\rm app}$
Type 1	0	0.74	0.45	0.68	0.35
Type 2	0	0.37	−0.12	0.41	−0.03
Type 3		0.49	0.04	0.49	0.09

TABLE V. Simulated orientational order parameters of Mitsui mixture for the chevron layer structure. The chevron angle was assumed at 15°. The other parameters were identical with Table III.

		40°C		60°C	
	σ_d (°)	$\langle P_2(\cos\beta)\rangle_{\rm app}$	$\langle P_4(\cos\beta)\rangle_{\rm app}$	$\langle P_2(\cos\beta)\rangle_{\rm app}$	$\langle P_4(\cos\beta)\rangle_{\rm app}$
Type 1	0	0.77	0.47	0.77	0.46
Type 2	0	0.42	−0.09	0.49	−0.01
Type 3		0.54	0.08	0.59	0.15

surface regions have very large space in the sample cell. However, the twisted structure that extends throughout the cell does not give a dark state. The thickness of the surface regions must be less than the wavelength of the visible light for obtaining the dark state at the tip of the V. Therefore, the polarization-stabilized twisted Sm*C** structure is inappropriate for the Mitsui mixture.

VI. DISCUSSION

In this way, the V-shaped switching is observed in both extremes of local in-plane director distributions at the tip of the V. One is considerably concentrated at a particular direction or two equivalent ones parallel to a plane perpendicular to the substrate plates, and the other is quite broadly distributed around the smectic layer normal. The former is described by Eq. (22) with a very small σ_d and the latter by Eq. (24). Two independent mechanisms may be possible to cause the two types of the V-shaped switching, which look apparently the same. However, both the compound (a) and the Mitsui mixture here investigated belong to a group of materials developed under the guiding principle of frustrating ferroelectricity and antiferroelectricity. These materials are closely related to the prototyped antiferroelectric liquid crystals, MHPOBC and TFMHPOBC, and have the quite similar molecular structures around the chiral centers. Moreover, our preliminary studies indicate that there exist some materials in which the distribution of the in-plane directors at the tip of the V is given by Eq. (22) with a large standard deviation σ_d [37]. Any distribution between both the extremes appears to be realized by an actual material. Consequently, it is natural to attribute a common cause for the V-shaped switching under consideration. When the director distribution is really concentrated, the charge stabilization and/or the highly collective azimuthal angle rotation of the local in-plane directors on the Sm*C** tilt cone in a macroscopic scale can meet the spatial uniformity during the V-shaped switching [16–20]. In the switching process from the electric-field-induced ferroelectric state to the one at the tip of the V, however, the highly collective azimuthal angle rotation in a macroscopic scale could hardly explain the spatial uniformity. It is general to anticipate domain formations due to the spatial irregularity on the substrate interfaces in the critical electric field at which the switching starts to occur. The same explanation does not hold for the quite broad distribution as in the Mitsui mixture, either.

Since the electric-field-induced continuous rotation of a spatially uniform optic axis characterizes the switching, the spatial nonuniformity of local in-plane directors must be restricted within regions smaller than the visible wavelength scale. What is essential to the V-shaped switching under consideration is the easy formation of invisible microdomains in case of need. This must be assured by the extreme softness with respect to the tilting directions and sense that results from the frustration between ferroelectricity and antiferroelectricity. This softness is also indicated by the phenomena of the phase destruction in a thin cell of the Mitsui mixture and of the very slow recovery from the state (alignment) dynamically realized at the tip of the V to the stable one at zero field in compound (a). An open question is whether the dynamic state is ferroelectric or not [19,38,39]? In previous papers, it was reported that the higher temperature phase above the antiferroelectric one is ferrielectric in compound (a) and the Inui mixture [3,4]. However, recent studies [36,37] indicate that it is peculiar ferroelectric Sm*C**. Because of the biaxial anchoring on polyimide aligning films, the so-called surface stabilized states becomes destabilized and the total anchoring energy of molecules on the Sm*C** tilt cone is almost independent of the azimuthal angle. Hence the relatively weak in-plane anchoring must force the molecules to align along the rubbing direction. In addition, the distribution around the rubbing direction may become broad when the twisting power is large. The biaxial anchoring of substrate interfaces destroy the antiferroelectric order and produce the broadly distributed alignment at zero dc field in the Mitsui mixture, which is clearly different from ordinary helical Sm*C** because no Goldstone mode is observed. The alignment at the tip of the V, also broadly distributed and almost described by Eq. (24), may be much closer to ordinary helical Sm*C**; the Goldstone mode may be observed by dynamically measuring the dielectric constant at the tip of the V [19]. The details of evolution from antiferroelectric to ferroelectric are future problems to be studied.

Finally, let us consider that the frustration between ferroelectricity and antiferroelectricity from a viewpoint of the free energy that is related with the interaction between the adjacent layers. Considering the symmetry of the phase, the averaged interlayer interaction can be represented in the following form with taking the first two Fourier components [40,41].

$$v(\Delta\phi) = v_1 \cos\Delta\phi - v_2 \cos 2\Delta\phi, \tag{31}$$

where $\Delta\phi$ is an azimuthal angle difference between the local in-plane directors of adjacent layers; $\Delta\phi=0$ and $\Delta\phi=\pi$ represent the synclinic and the anticlinic orderings, respectively. A small deviation due to the helicity is ignored. Positive v_1 promotes the anticlinic ordering while v_2 represents

the energy barrier between synclinic and anticlinic ordering. The distribution of the local in-plane directors critically depends on the barrier v_2. The small v_1 and relatively large v_2 compared with the thermal agitation give a long relaxation time from synclinic to anticlinic ordering. Therefore, the synclinic ordering is conserved under periodically applied electric field at an appropriate frequency for the V-shaped switching. The electric-field-induced ferroelectric state, which is characterized with a small distribution of the in-plane directors, may rotate almost collectively because the total anchoring energy on the SmC^* tilt cone is nearly independent of the azimuthal angle [16–23,36,37]. This is actually observed in compound (a). When v_2 is sufficiently small so that the substrate interfaces destroy the anticlinic, antiferroelectric structure [14,36,37], the thresholdless switching occurs even in the first run as actually observed in the Mitsui mixture. Moreover, the spatial irregularity on the substrate interfaces, together with the strong twisting power, may promote the large distribution of ϕ during the V-shaped switching. This type of the switching corresponds to the Mitsui mixture.

VII. CONCLUSIONS

Polarized Raman scattering technique is very useful for the evaluation of orientational molecular distribution in liquid crystal systems. The orientational order parameters were investigated for two types of liquid crystals showing the V-shaped switching, compound (a) and Mitsui mixture. The results showed two extreme distributions of the local in-plane director at the tip of the V. The compound (a) exhibited a small distribution, while the Mitsui mixture exhibited a large distribution. The small distribution of the local in-plane directors for the compound (a) suggests the collective azimuthal angle rotation in the V-shaped switching process. However, the same explanation does not hold for the Mitsui mixture with quite large distribution of the local in-plane directors at the tip of the V. What is essential to the V-shaped switching is the easy formation of invisible microdomains in case of need. This required the softness with respect to the tilting directions and sense that results from the frustration between ferroelectricity and antiferroelectricity. The difference in the distribution of two types of liquid crystals at the tip of the V was explained by the barrier between synclinic and anticlinic ordering in adjacent layers. The small barrier gave a large distribution at the tip of the V in the dynamic switching, consequently triggered the V-shaped switching even in the firstrun. On the other hand, the large barrier did a small distribution and the tristable switching.

ACKNOWLEDGMENTS

We would like to thank Mitsui Chemicals, Inc. and Nissan Chemical Industries, Ltd. for supplying the liquid crystal and aligning polyimide samples used. This work was partially supported by a Grant-in-Aid for Scientific Research (No. 12650010) from the Japan Society of the Promotion of Science and by the Joint Studies Program (2001-2002) of the Institute for Molecular Science.

[1] C. Tanaka, T. Fujiyama, T. Maruyama, and S. Nishiyama, in *Abstracts of 1995 Japanese Liquid Crystal Conference, Sendai, Japan* (Japanese Liquid Crystal Society, Tokyo, 1995), p. 250.

[2] A. Fukuda, in *Proceedings of the 15th International Display Research Conference (Asia Display '95), Hamatsu, Japan* (Society for Information Display, San Jose, CA, 1995), p. 61.

[3] T. Matsumoto, A. Fukuda, M. Johno, Y. Motoyama, T. Yui, S.-S. Seomun, and M. Yamashita, J. Mater. Chem. **9**, 2051 (1999).

[4] M. Takeuchi, K. Chao, T. Ando, T. Matsumoto, A. Fukuda, and M. Yamashita, Ferroelectrics **246**, 1 (2000).

[5] S. Inui, N. Iimura, T. Suzuki, H. Iwase, K. Miyachi, Y. Takanishi, and A. Fukuda, J. Mater. Chem. **6**, 671 (1996).

[6] L.K.M. Chan *et al.*, in *Proceedings of the 20th International Display Research Conference (IDRC '00), Plam Beach, Florida* (Society for Information Display, San Jose, CA, 2000), p. 261.

[7] T. Yoshida, J. Ogura, M. Takei, H. Wakai, and H. Aoki, in *Conference Summaries of the 7th International Conference on Ferroelectric Liquid Crystals (FLC '99), Darmstadt, Germany* (Darmstadt University of Technology, Germany, 1999), p. 138.

[8] J. Ogura, T. Yoshida, M. Takei, H. Wakai, and H. Aoki, in *Proceedings of the IDW '99 Digest, Sendai, Japan* (Society for Information Display, San Jose, CA, 1999), p. 199.

[9] T. Yoshida, J. Ogura, M. Takei, N. Yazawa, R. Mizusako, S. Ando, H. Wakai, and H. Aoki, in *Proceedings of the 7th International Display Workshops (IDW '00), Kobe, Japan* (Society for Information Display, San Jose, CA, 2000), p. 37.

[10] R. Hasegawa, H. Yamaguchi, R. Fukushima, and K. Takatoh, in *Conference Summaries of the 7th International Conference on Ferroelectric Liquid Crystals (FLC '99), Darmstadt, Germany* (Darmstadt University of Technology, Germany, 1999), p. 102.

[11] R. Hasegawa, H. Fujiwara, H. Nagata, Y. Hara, T. Saishu, R. Fukushima, M. Akiyama, H. Okumura, and K. Takatoh, J. Soc. Inf. Dis. **9**, 107 (2001).

[12] S.S. Seomun, Y. Takanishi, K. Ishikawa, H. Takezoe, and A. Fukuda, Jpn. J. Appl. Phys., Part 1 **36**, 3586 (1997).

[13] S.-S. Seomun, T. Gouda, Y. Takanishi, K. Ishikawa, H. Takezoe, and A. Fukuda, Liq. Cryst. **26**, 151 (1999).

[14] D. Pociecha, M. Glogarova, E. Gorecka, and J. Mieczkowski, Phys. Rev. E **61**, 6674 (2000).

[15] P.E. Cladis and H.R. Brand, Ferroelectrics **213**, 63 (1998).

[16] H. Takezoe, A.D.L. Chandani, S.S. Seomun, B. Park, D.S. Hermann, Y. Takanishi, and K. Ishikawa, in *Proceedings of the 18th International Display Research Conference (Asia Display '98), Seoul, Korea* (Society for Information Display, San Jose, CA, 1998), p. 106.

[17] B. Park, S.S. Seomun, M. Nakata, M. Takahashi, Y. Takanishi,

K. Ishikawa, and H. Takezoe, Jpn. J. Appl. Phys., Part 1 **38**, 1474 (1999).
[18] B. Park, M. Nakata, S.S. Seomun, Y. Takanishi, K. Ishikawa, and H. Takezoe, Phys. Rev. E **59**, R3815 (1999).
[19] P. Rudquist, *et al.*, J. Mater. Chem. **9**, 1257 (1999).
[20] N.A. Clark, D. Coleman, and J.E. Maclennan, Liq. Cryst. **27**, 985 (2000).
[21] S.S. Seomun, T. Fuukuda, A. Fukuda, J.G. Yoo, Y.P. Panarin, and J.K. Vij, J. Mater. Chem. **10**, 2791 (2000).
[22] S.S. Seomun, J.K. Vij, N. Hayashi, T. Kato, and A. Fukuda, Appl. Phys. Lett. **79**, 940 (2001).
[23] S.S. Seomun, V.P. Panov, J.K. Vij, A. Fukuda, and J.M. Oton, Phys. Rev. E **64**, 040701 (2001).
[24] S. Jen, N.A. Clark, and P.S. Pershan, Phys. Rev. Lett. **31**, 1552 (1973).
[25] S. Jen, N.A. Clark, P.S. Pershan, and E.B. Priestley, J. Chem. Phys. **66**, 4635 (1977).
[26] C.H. Wang, *Spectroscopy of Condensed Media* (Academic, London, 1985).
[27] N. Hayashi and T. Kato, Phys. Rev. E **63**, 021706 (2001).
[28] N. Hayashi, T. Kato, T. Aoki, T. Ando, A. Fukuda, and S.-S. Seomun, Phys. Rev. Lett. **87**, 015701 (2001).
[29] M. Lax and D.F. Nelson, Phys. Rev. B **4**, 3694 (1971).
[30] M. Lax and D.F. Nelson, J. Opt. Soc. Am. **65**, 668 (1975).
[31] R. Akiyama, M. Hasegawa, A. Fukuda, and E. Kuze, Jpn. J. Appl. Phys. **20**, 2019 (1981).
[32] G.-P. Chen, H. Takezoe, and A. Fukuda, Jpn. J. Appl. Phys., Part 1 **28**, 56 (1989).
[33] B. Wen, S. Zhang, S.S. Keast, M.E. Neubert, P.L. Taylor, and C. Rosenblatt, Phys. Rev. E **62**, 8152 (2000).
[34] S. Zhang, B. Wen, S.S. Keast, M.E. Neubert, P.L. Taylor, and C. Rosenblatt, Phys. Rev. Lett. **84**, 4140 (2000).
[35] M. Johno, Y. Ouchi, H. Takezoe, A. Fukuda, K. Terashima, and K. Furukawa, Jpn. J. Appl. Phys., Part 2 **29**, L111 (1990).
[36] T. Matsumoto, Y. Suzuki, M. Johno, T. Okugawa, M. Takeuchi, and A. Fukuda, Jpn. J. Appl. Phys., Part 2 **40**, L817 (2001).
[37] A. Fukuda, H. Hakoi, T. Okugawa, T. Ando, T. Matsumoto, Y. Suzuki, M. Johno, N. Hayashi, T. Kato, S. Kawada, and S. Kondoh, in *Proceedings of the 21st International Display Research Conference in conjunction with the 8th International Display Workshops (Asia Display/IDW '01), Nagoya, Japan* (Society for Information Display, San Jose, CA, 2001), p. 77.
[38] M. Johno, K. Itoh, J. Lee, Y. Ouchi, H. Takezoe, A. Fukuda, and T. Kitazume, Jpn. J. Appl. Phys., Part 2 **29**, L107 (1990).
[39] K. Hiraoka, A.D.L. Chandani, E. Gorecka, Y. Ouchi, H. Takezoe, and A. Fukuda, Jpn. J. Appl. Phys., Part 2 **29**, L1473 (1990).
[40] M.A. Osipov and A. Fukuda, Phys. Rev. E **62**, 3724 (2000).
[41] T. Qian and P.L. Taylor, Phys. Rev. E **60**, 2978 (1999).